



BR98E1510

* INFORMAÇÕES SOBRE O PREÇO DE VENDA DO MATERIAL DEBEM SER CONSULTADAS NO LOCAL DE AQUISIÇÃO *

**MEDIUM CARBON VANADIUM
MICROALLOYED STEELS FOR DROP
FORGING**

**Gábor Jeszensky
Ronald Lesley Plaut**

São Paulo, 1992

36483
IPT
Pub. 1989
e.s.
013363-19



R

29 - 42

**We regret that
some of the pages
in this report may
not be up to the
proper legibility
standards, even
though the best
possible copy was
used for scanning**

ABSTRACT

Growing competitiveness of alternative manufacturing routes requires cost minimization in the production of drop forged components. The authors analyse the potential of medium carbon, vanadium microalloyed steels for drop forging.

Laboratory and industrial experiments have been carried out emphasizing deformation and temperature cycles, strain rates and dwell times showing a typical processing path, associated mechanical properties and corresponding microstructures.

The steels obtain the required levels of mechanical properties on cooling after forging, eliminating subsequent heat treatment.

The machinability of V-microalloyed steels is also improved when compared with plain medium carbon steels.

1. INTRODUCTION

The technological challenge within the traditional drop forging industry has been characterized by its multiplicity since it has to compete with alternative manufacturing processes as casting and materials such as aluminium alloys, glass fibers and carbon fibers, going to the extent to attend demanding markets where components of higher performance and lower prices are required.

It is generally recognized that the mechanical properties, toughness, ductility and fatigue life of cast components are inferior to forged steels. Forgings must therefore remain as "first choice" production method for applications where a high strength-to-weight ratio combined with ductility and fracture toughness is mandatory.

Hardened and tempered forgings are used for severely stressed engineering components and cannot be surpassed for performance, reliability, fatigue resistance and tolerance to unpredicted overloading. However, there are some applications where designers have been able to use cast iron without significant incidence of failures; clearly, in such applications there is no need for impact toughness or ductility. Between these extremes there is room for steel forgings of high strength with toughness and ductility values somewhat lower than for hardened and tempered steel, but greatly superior to those of cast iron. Such forgings are cooled under controlled conditions after the forging operation and are not heat-treated subsequently. In addition to energy saving, this may also eliminate the need for straightening and stress-relieving with their attendant problems.

From the machinability point of view, a more effective utilization and selection of cutting tools and/or the use of improved machinable steels can lead to increased productivity during final shaping by metal cutting.

In hot-rolled structural steels (with carbon contents up to 0.20%) it has been well documented that tensile properties can be improved by grain refinement and/or precipitation hardening, by making "micro-alloying" additions of elements such as niobium or vanadium (1).

Generally, the maximum degree of grain refinement is sought, as this improves ductility and toughness also, whereas precipitation hardening is detrimental to both these properties.

The benefits to be obtained by microalloying additions to low carbon steels hot rolled into sheet and plate have been known and utilized for some time (1).

The process of hot forging is one of thermal-mechanical treatment. Therefore the properties of the as-received hot rolled bars are significantly altered during forming.

Traditionally, the desired properties in most critical automotive parts have been obtained by heat treatment.

However, microalloying medium carbon steels for forging applications has permitted the elimination of heat treatment in some cases. Forgings receive more variable deformation and cooling than are experienced during the hot rolling of sheet and plate. However, the concerns appropriate to the hot rolling of microalloyed steels are the same to be considered in forging microalloyed steels.

Developments in Europe (2), USA (3) and Japan (4) applied the "Micro-Alloying" concepts in the last five years to the strengthening of medium carbon steels (0.45 - 0.60%) for the forging of automotive components.

On air-cooling such steels, the structure consists of pearlite and ferrite, and the strength is enhanced by precipitation of vanadium and/or niobium carbonitrides.

From the literature, it is clear that grain refinement of medium carbon steels with precipitates is not possible as the solubility of niobium at billet soaking temperatures is very low. Hence, only a very small volume fraction of niobium carbonitride would be available for precipitation during hot working (5). Vanadium carbonitride, on the other hand, would be readily soluble at soaking temperatures, but remain in solution at the austenite-ferrite transformation temperature (6). Therefore, the enhancement of strength relies solely on the precipitation of vanadium carbonitride, the strength increment being dependent of the volume fraction and particle size of the precipitate.

2. STRUCTURE / PROPERTY RELATIONSHIPS

The structure/property relationships in ferrite/pearlite steels are summarised in the equations of Gladman and others (7).

$$R_{el} = f_{\alpha}^{1/3} (35.4 + 58.5 (\% \text{ Mn}) + 17.4 d^{-1/2}) + (1 - f_{\alpha}^{1/3}) (178.6 + 3.85 S_o^{-1/2}) + 63.1 (\% \text{ Si}) + 425 (\sqrt{\% \text{ N}}) \quad (\text{I})$$

$$R_m = f_{\alpha}^{1/3} (246.4 + 1142.7 (\sqrt{\% \text{ N}}) + 18.7 d^{-1/2}) + (1 - f_{\alpha}^{1/3}) (719.2 + 3.54 S_o^{-1/2}) + 15.8 (\% \text{ Si}) \quad (\text{II})$$

Where,

- R_m = UTS (N/mm^2)
- R_{el} = Y.S. (0,2%), (N/mm^2)
- d = Ferrite grain size (mm)
- f_{α} = Volume fraction of ferrite
- $1-f_{\alpha}$ = Volume fraction of pearlite
- S_o = True mean interlamellar spacing of pearlite (mm)
- N = "Free" nitrogen content in solid solution
- Mn = Manganese in %
- Si = Silicon in %

The microstructural parameters in equations (I) and (II) which determine the mechanical properties, i.e., ferrite content, grain size, interlamellar spacing etc, are all controlled by three processing variables, i.e. composition, prior austenite grain size (and therefore finishing forging temperature) and the cooling rate after forging. In fact, the effects of these processing variables are inter-related to a large extent and often cannot be considered independently..

These equations do not take into account the precipitation strengthening contribution but this can be determined by the difference between actual and predicted values, and accounted for from the evaluation of the soluble microalloying element, as shown by Brandis (15) and discussed later on.

Some typical compositions , metallographic data and mechanical properties for several vanadium microalloyed steels are given in tables 1 and 2.

A typical CCC diagram for those steels is presented in fig. 1.

Figure 2 and 3 show typical optical microstructures for vanadium microalloyed steels, respectively cooled in still air and forced air. Figures 4 to 6 present some typical electron microscopies of ferrite (cooled in still air), pearlite (cooled in still air) and ferrite (cooled in forced air). In all these it is important to stress the size of the particles of ~ 10 nm ($0,010$ μ m).

A typical Charpy impact energy transition curve for a vanadium treated steel is shown in fig. 7.

It indicates a fracture appearance transition temperature (FATT) of around 100°C . Hence, at ambient temperature the steels exhibit largely brittle fracture characteristics in the Charpy test. A significant improvement in toughness at room temperature can only be achieved, therefore, by a decrease in FATT of about 100°C . In order to decrease FATT by this order of magnitude, an ultra-fine austenite grain size is required and this is extremely difficult to achieve in air-cooled medium carbon steels, after forging and finishing at usually high temperatures.

For many components, such as crankshafts and connecting rods, there is not a critical requirement for toughness and vanadium microalloyed steels are specially suitable. It should be pointed out that, although microalloyed steels are apparently inferior in terms of impact resistance, this parameter is useful for hardened and tempered grades purely in terms of quality control, as it is extremely effective in identifying unsatisfactory batches of material. However, impact properties are of no relevance in relation to the operating conditions for many components and therefore, the same criteria should not necessarily be used for the quality control of a new type of material, such as microalloyed steel. For example, during the development of these steels, several European and Japanese Automotive Manufacturers have been able to establish that microalloyed steel crankshafts and connecting rods are perfectly satisfactory under running conditions. It seems reasonable to conclude that impact properties are not of prime importance in components of this type, which normally fail by fatigue.

It has been pointed out by Whittaker (8) that on cyclic testes carried out on both hardened and tempered and on microalloyed steels, cyclic softening was typical of the former ones whereas the latter did not show such a behavior . More recent work on fatigue tests carried out on samples forged from microalloyed steel presented virtually identical behavior to the hardened and tempered samples, with similar tensile strength level (9).

On machinability it has been found that microalloyed steels produce substantially lower tool wear rates and longer tool lives when compared to conventional steels quenched and tempered to similar strength levels (fig. 8 and 9). Benefits have been observed with both turning and drilling operations. This improved machinability may be attributed to the ferrite/pearlite microstructure, wich is more desirable than a tempered ferrite/carbide structure present in conventional heat-treated steels. Further benefits to tool life are also realized by adoption of enhanced sulphur levels with superior surface finish and swarf-removal characteristics (up to about 0.07%), according to (12).

3. PROCESSING VARIABLES

Forging of V-Microalloyed steels, taken as a thermomechanical treatment, presents some important processing variables, which have been already studied by some authors, variables such as heating temperature, finishing temperature and cooling rate.

Bucher (10) pointed out the effect of heating temperature on the hardness of forgings as shown in figure 10.

Niwa (11), Bucher (10) and Thewlis (12) have shown that for the best strength toughness results, a soaking temperature of 1200 - 1300°C and a cooling rate of about 100°C/minute or slightly faster would be recommended, figure 11.

Thewlis (12), Baffigi et al (9) showed that some improvement on ductility and toughness, but not so significant on strength is obtained due to austenite grain refinement through diminishing forging temperatures, as shown in figure 12.

Nippon steel has reported (13) that a Carbon Equivalent = $(C + Mn/5 + Si/7 + Cr/3 + V/2)$, should be selected for various forged parts to achieve the desired hardness using air cooling and a reheating temperature in the range of 1200 - 1300° C, as shown by figure 13.

4. OBJECTIVES

Based upon the information available in the literature, briefly summarized above, it is the intention to present here part of a continuous research programme carried out both at laboratory scale (I.P.T. S/A) and at industrial conditions (SIFCO S/A), namely the forging of connecting rods and front axles.

5. TESTS AND EXPERIMENTAL RESULTS

5.1 Materials

The chemical composition of the materials employed in this work are given in table 3.

The carbon equivalent, for this V-Microalloyed steel, is 0.792.

For the production of connecting rods and front axles the original rolled billet square sections were 38.1 mm and 95.0 mm, respectively.

5.2 Experimental Conditions

For the laboratory work a 1500 ton. hydraulic press supported by a Globar heating furnace has been used whereas a 40 T x m power drop hammer together with a conventional oil furnace have been employed for the production of front axles and a 1300 ton. hydraulic press in conjunction with induction heating for the forging of connecting rods. Cooling has been in still air and in vermiculite.

5.2.1 Laboratory Tests

Cylindrical samples (\emptyset 38.0 X 55.0 mm) have been deformed for varying reductions of 30%, 50% and 70% at two temperatures namely 1200°C and 1050°C. Temperature control through embedded thermocouples and cross-head speed have been recorded for all experiments. The measured experimental strain rate was of 0.43 S^{-1} .

5.2.2 Industrial Tests

For the forging parts under consideration during hot working, the time, temperature and deformations, during the different forging phases, on specific sections associated with extreme deformations, have been monitored. The measured average strain rate in this case, was of $0,5 \text{ S}^{-1}$.

5.3 Experimental Results

Table 5 summarizes the microstructures of laboratory results, for the different conditions studied:

Grain refinement, as expected, is obtained for larger reductions, faster cooling rates and lower reheating temperatures.

Figure 14 shows the typical evolution of deformations and temperatures observed during the forging of connecting rods.

A similar diagram has been obtained for the front axles, as shown in figure 15.

In figure 14 the microstructure at the three main cross sections of the connecting rod are also shown for the forging temperatures at 1250°C and 1100°C . Here it must be pointed out the significantly different deformation path for the sections studied leading to the different observed microstructures. Starting at lower forging temperatures lead to approximately similar finishing temperatures, due to adiabatic heating, hence similar microstructures.

Figure 16 shows the hardness distribution for the main sections of the connecting rod. Despite different initial forging temperatures and final deformations, varying for different sections, the hardness distribution has been relatively uniform.

The experimental cooling rate obtained was in the range of $150 - 400^{\circ}\text{C} / \text{minute}$.

In the case of front axles, figure 17, shows the hardness distribution being again fairly uniform.

In this case the experimental cooling rate was $25^{\circ}\text{C}/\text{minute}$.

Table 4 shows the mechanical properties obtained from samples taken from section "A" of the front axle.

Machinability tests have been carried out on samples taken from the original billets applying the AFNOR A03-654 testing specifications. When comparing conventional SAE 1046 (Q + T) with V-Microalloyed steels the results show a 25% improvement in machinability in the latter case.

Intensive fatigue testing is at present under consideration using the bench test technique for front axle components, encouraged by positive results obtained by other investigators (17).

6. DISCUSSION

According to Gladman (7), the solubility limits of VN and VC are given by:

$$\text{Log}_{10} = [V] \cdot [N] = \frac{-8330}{T \text{ (°K)}} + 3.46$$

$$\text{Log}_{10} = [V^{4/3}] \cdot [C] = \frac{-10800}{T \text{ (°K)}} + 7.06$$

or according to Brandis (15):

$$\text{Log}_{10} = [V] \cdot [N] = \frac{-5996}{T \text{ (°K)}} + 1.80$$

For the V-Microalloyed steel under consideration, where V = 0.15 wt%, C = 0.45 wt% and N = 0.007 wt%, the temperatures for a complete solubility of vanadium, would be, according to these equations, 1020°C, 996°C and 980°C, respectively, showing that for all the experimental conditions V has been taken into solution.

For the carbon equivalent of 0.792, according to figure 13 the experimental hardness values are slightly higher than those indicated, yet if the figure 11 is considered for the respective cooling rates, of 25° C/minute (front axle) and 150 - 400°C/minute (connecting rod) the hardness values are compatible with the experimental results for these forgings.

The experimental results showed that despite variations in deformation and cooling rate, for various forging cross sections the hardness distribution has been fairly uniform as could be expected from the flat topped CCC curve for the V-Steel, shown in figure 1.

Structure refinement can be obtained mainly by increased deformation and also by lowering the final deformation temperature but leading to an increase in ferrite content and hence reduced pearlite percentage which is both beneficial to ductility and toughness as shown by Baffigi et al (9) and confirmed by the laboratory tests.

If we take table 5 it is possible to observe that for "normal" forging temperatures and deformations ferrite grain size is about 20 μm and that the pearlite volume fraction is $\sim 90\%$. From figure 18 we take a typical interlamellar spacing of $\sim 400 \mu\text{m}$. If we take these values into consideration in Gladman's equation (I) the calculations indicate that the precipitation strengthening contribution for the steel studied is in the order of 270 N/mm^2 which is in accordance with the values given in table 2 and with Brandis (15) experimental observations, shown in figure 19.

In fact, at finishing forging temperatures of 900°C for the connecting rods, according to Brandis (16) about 0.12% V would be in solution (and available for precipitation on cooling)(14); hence from fig. 19 we would have a contribution due to precipitation strengthening of the order previously indicated. Brandis also points out that this contribution would be greater from the coherent "clusters" than from the electron microscope visible, incoherent $\sim 10 \text{ nm}$ particles as shown in fig. 4 to 6.

The improved machinability index of the V-Microalloyed steel, when compared to the conventional SAE 1046 (Q + T), is mainly associated to the fact that the former does not have any tempered martensite structure.

7. CONCLUSIONS

In terms of forgeability the V-Microalloyed medium carbon steels compares well with the plain medium carbon steels.

Tensile and yield strengths for V-Microalloyed steels showed higher values whereas ductility and toughness presented somewhat lower values when compared to plain medium carbon steels. This disadvantage is not really significant in the case of connecting rods and other components where the fatigue performance required can be overcome, as pointed out by Gladman's Equation, by refining ferrite grain and pearlite colony sizes, and volume fractions and proper control of the V additions can further enhance tensile and yield stress values. These variables can be adjusted, through an adequate thermomechanical treatment, i.e. larger deformation at lower finishing temperatures and faster cooling rates as demonstrated both by the laboratory and industrial trials.

The fine ferrite pearlite microstructure obtained shows a 25% increase in machinability when compared to quenched and tempered plain medium carbon steels.

As an alternative forging material it is also possible to obtain cost reduction of a forged component by avoiding conventional heat treatment in addition to the fact that the as forged component does not require straightening.

ACKNOWLEDGEMENTS

The authors acknowledge Dr. Alexandre R. S. Vasconcellos, President of SIFCO S/A and of the Brazilian Forging Association, CBF, for the constant stimulation and support throughout the work as well as for the permission to publish the present paper. The help of Mr. L. P. R. Segalla from SIFCO S/A and of Mr. E. A. Simielli from I.P.T. S/A throughout the experimental work is also acknowledged.

REFERENCES

- (1) F. B. PICKERING - Proc. Conference "Microalloying 75"; Ed. M. Korchynsky, 1975, N. York, p. 9.
- (2) A.V. STEINEN et al - Stahl und Eisen - 95 - 1975 - N6 - March, p. 209.
- (3) J. H. BUCHER - Niobium Conference, 1981, p. 989.
- (4) H. HASIMOTO et al - SAE Paper NR. 820125 - February 1982.
- (5) H. BRANDIS et al - Thyssen Tech. BER - 1978, Vol I, p.3
- (6) F. B. PICKERING - Conf. HSLA Steels technology and Applications - Ed. M. Korchynsky - 1983, N. York, p. 1.
- (7) T. GLADMAN et al - J.I.S.I. - December 1972, p. 916.
- (8) D. WITTAKER - Metalurgia - April 1979, p. 275.
- (9) N. BAFFIGI et al - Metallurgical Science and Technology, Vol. 3 (2), 1985, p. 55.
- (10) J. H. BUCHER - Proceedings on Speciality Steels and Hard Materials, South Africa, 8 - 12 Nov. 1982.
- (11) S. NIWA et al - SAE Paper NR. 810426, 1981.
- (12) G. T. THEWLIS et al - Metals and Materials, December 1981, p. 21.
- (13) Nippon Steel Corporation (1982) - "Microalloyed Steel Bars for as Hot Forged", as ref. cit. - in (10).
- (14) T. GLADMAN et al - Proceedings of conference on "Microalloying 1975", Ed. M. Korchynsky, 1975, p. 32.

- (15) H. BRANDIS et al - Thyssen Edel. Tech. Ber V. 4 - NI - 1978 - p. 3.
- (16) H. BRANDIS et al. - HTM - 1981 - V. 3 - p. 134.
- (17) R. W. THOMPSON - Proc. 22nd Mech. Working and Steelmaking Conference - Toronto, AIMME, Oct. 1980, p. 75.

T A B L E S A N D F I G U R E S

- TABLE 1 : Chemical composition of microalloyed steels, 49MnVS3 and Vanard.
- TABLE 2 : Metallographic and property data for Vanard steels and 49MnVS3.
- TABLE 3 : Chemical composition of SAE 1046 and vanadium steel VB.
- TABLE 4 : Shows the mechanical properties obtained from samples taken from section "A" of the front axle.
- TABLE 5 : Microstructure of samples from laboratory trials.
-
- FIGURE 1 : Typical continuous cooling diagram for a medium carbon, vanadium microalloyed steels. Ref. 2.
- FIGURE 2 : Microstructure of vanadium microalloyed steel (air cooled).(100x).
- FIGURE 3 : Microstructure of vanadium microalloyed steel (forced air cooled). (100x).
- FIGURE 4 : Electron microscopy of V(C,N) in ferrite, cooled in still air. (5000x). Ref. 2.
- FIGURE 5 : Electron microscopy of V(C,N) in ferrite of pearlite, cooled in still air. (10000x). Ref. 2.
- FIGURE 6 : Electron microscopy of V(C,N) in ferrite, forced air cooled. (5000x). Ref.2.
- FIGURE 7 : Typical Charpy energy transition curve (V-steel). Ref. 12.
- FIGURE 8 : Tool wear of Vanard 1100S and 708M40 (EN 19). Ref. 12.

- FIGURE 9 : Tool life, selected steels. Ref. 12.
- FIGURE 10 : The effect of heating temperature on the hardness of forgings.
Ref. 10.
- FIGURE 11 : Effect of cooling rate on the hardness of forgings. Ref. 10.
- FIGURE 12 : Effect of forging temperature on the grain size of forgings.
Ref. 9..
- FIGURE 13 : Effect of carbon equivalent on the hardness. Ref. 13.
- FIGURE 14 : Typical deformation and temperature path of connecting rod..
Structure distribution for main sections of the connecting rod.
(200 x).
- FIGURE 15 : Typical deformation and temperature path for the "A" section
of the forged front axle.
- FIGURE 16 : Hardness distributions for main sections of the connecting rod.
(Hv).
- FIGURE 17 : Hardness distribution for section "A" of the front axle (Hv).
- FIGURE 18 : Typical S.E.M. of pearlite.
- FIGURE 19 : Effect of Vanadium additions on 0,2% Y.S. Ref. 15.

T A B L E 1

TYPE	C	Si	Mn	P	S	V	(wt%)
49MnVS3	0.42/0.50	0.60 máx.	0.60/1.00	0.035 máx.	0.045/0.065	0.08/0.13	
Vanard	0.30/0.50	0.15/0.35	1.00/1.50	0.035 máx.	0.050 máx.	0.05/0.20	

TABLE 1 : Chemical composition of microalloyed steels; 49MnVS3 and Vanard.

TABLE 2

METALLOGRAPHIC AND PROPERTY DATA FOR VANARD STEELS AND 49 Mn VS3												
STEEL	METALLOGRAPHIC DATA						PREDICTED PRECIPITATION STRENGTHENING		ACTUAL MECHANICAL PROPERTIES			
	ASTM GRAIN SIZE N ^o	PEARLITE %	FERRITE GRAIN SIZE μm	PEARLITE COLONY SIZE μm	INTER-LAMELLAR SPACING PEARLITE nm	AVERAGE CEMENTITE LATH THICKNESS nm	ΔYS N/mm ²	ΔTS N/mm ²	YIELD STRENGTH N/mm ²	TENSILE STRENGTH N/mm ²	EI %	YS/TS RATIO
49 Mn VS3	5.0	77	8.3	16.5	294	35.5	210	209	570	895	14	0.64
VANARD 850	6.5	73	5.8	13.2	283	48.6	216	182	604	865	20	0.70
VANARD 925	6.5	87	4.3	13.9	276	48.0	229	184	648	944	20	0.69
VANARD 1000	5.5	94	3.0	12.6	279	43.5	246	167	692	1001	16	0.69
VANARD 1100	6.5	91	3.1	13.1	266	40.1	393	307	842	1122	16	0.75
0.2 % PROOF STRESS † FREE NITROGEN 0.001												

T A B L E 3

TYPE	C	Mn	Si	P	S	V	N	(wt%)
SAE 1046	0.45	0.86	0.27	0.030	0.019	-	0.009	
VB	0.45	1.13	0.29	0.014	0.029	0.15	0.007	

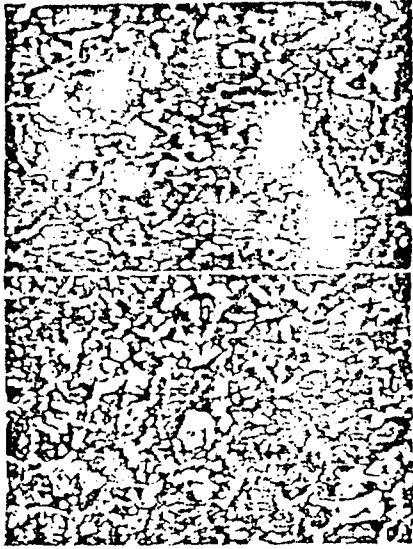

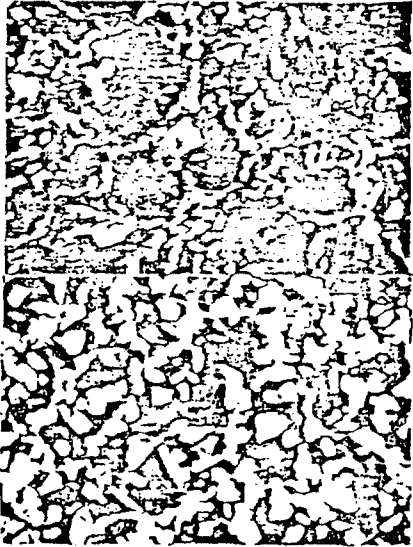
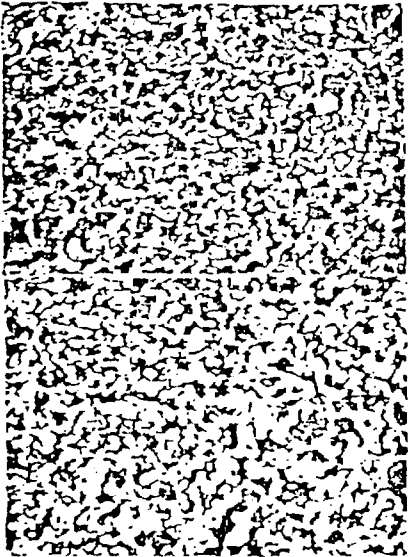
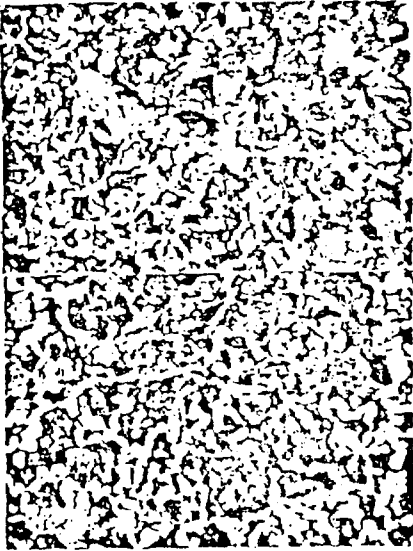
TABLE 3 : Chemical composition of SAE 1046 and vanadium steel VB.

6T - 8 - IIA

T A B L E 4

TEST	T. S. <i>kgf/mm²</i>	Y. S. <i>kgf/mm²</i>	ELONGAT. %	REDUCT. IN AREA %	IMPACT (20°C) (J)
STEEL					
MICROALLOYED	98	64	12	22	10
SAE 1046 M	84	53	23	56	16

TABLE 5

<p>r = 30% (ε = 0.4)</p>		 <p>A</p> <p>V</p>
<p>r = 50% (ε = 0.7)</p>	 <p>A</p> <p>V</p>	 <p>A</p> <p>V</p>
<p>r = 70% (ε = 1.2)</p>	 <p>A</p> <p>V</p>	 <p>A</p> <p>V</p>

A- air

V= vermiculite

100x

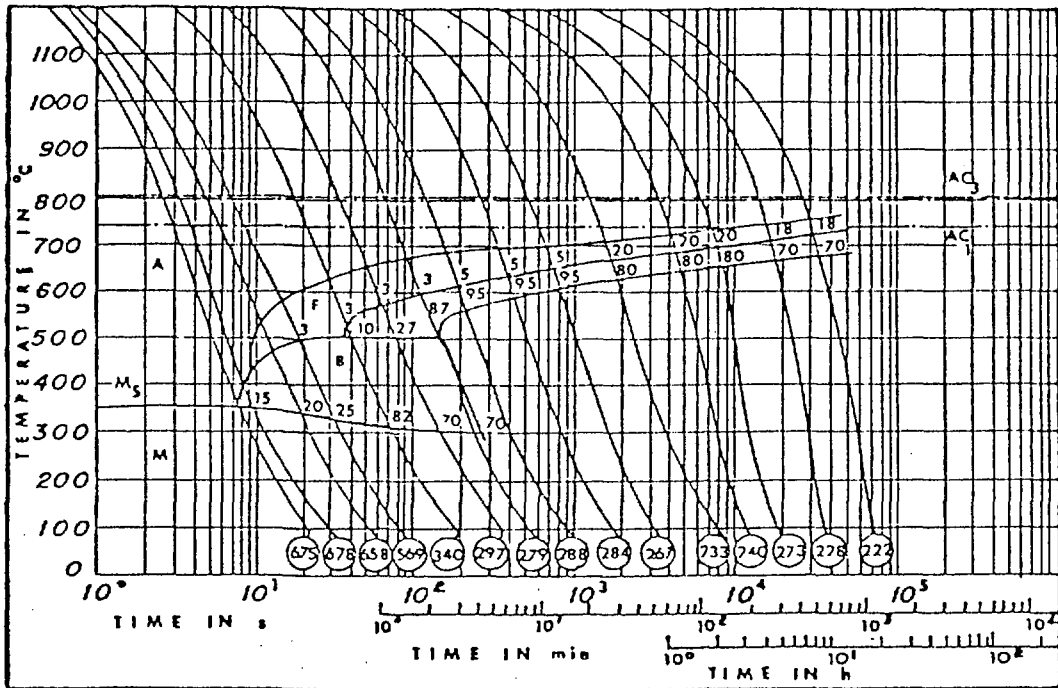


FIGURE 1 : Typical continuous cooling diagram for a medium carbon, vanadium microalloyed steels. Ref. 2.

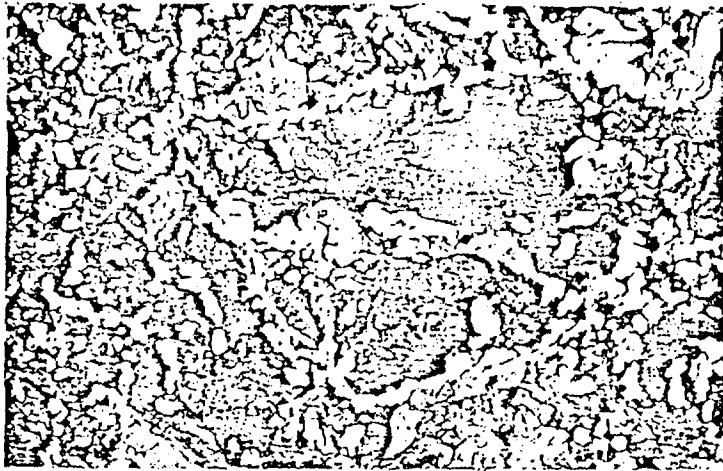


FIGURE 2 : Microstructure of vanadium microalloyed steel (air cooled). (100x).



FIGURE 3 : Microstructure of vanadium microalloyed steel (forced air cooled). (100x).

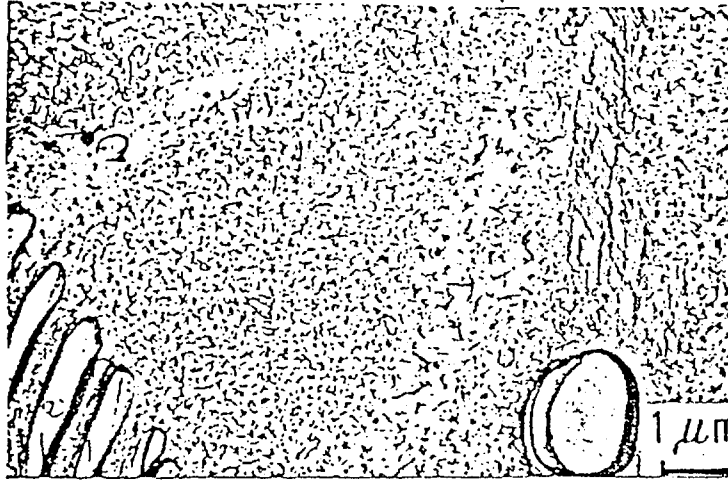


FIGURE 4 : Electron microscopy of V(C,N) in ferrite, cooled in still air (5000x). Ref.2.

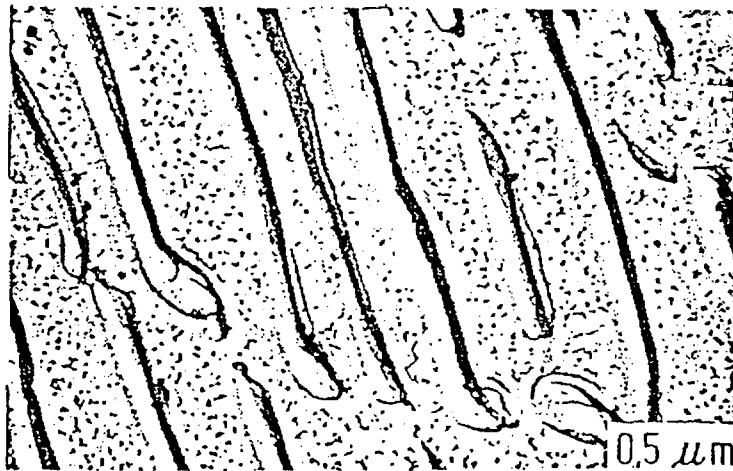


FIGURE 5 : Electron microscopy of V(C,N) in ferrite of pearlite, cooled in still air (10000x). Ref.2.

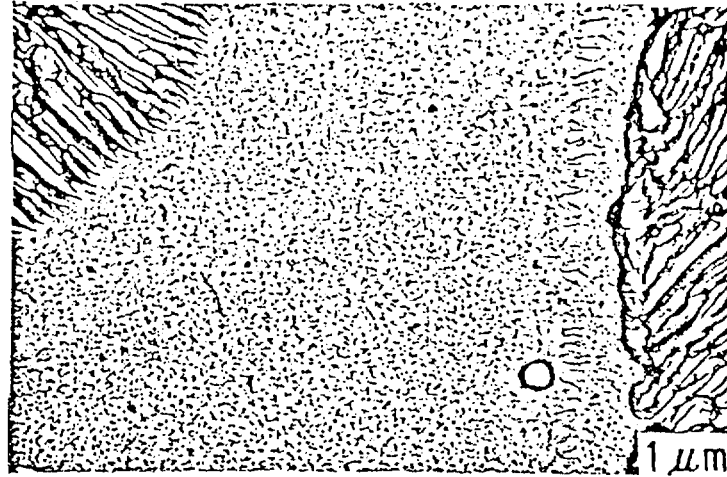


FIGURE 6 : Electron microscopy of V(C,N) in ferrite, forced air cooled. (5000x). Ref. 2.

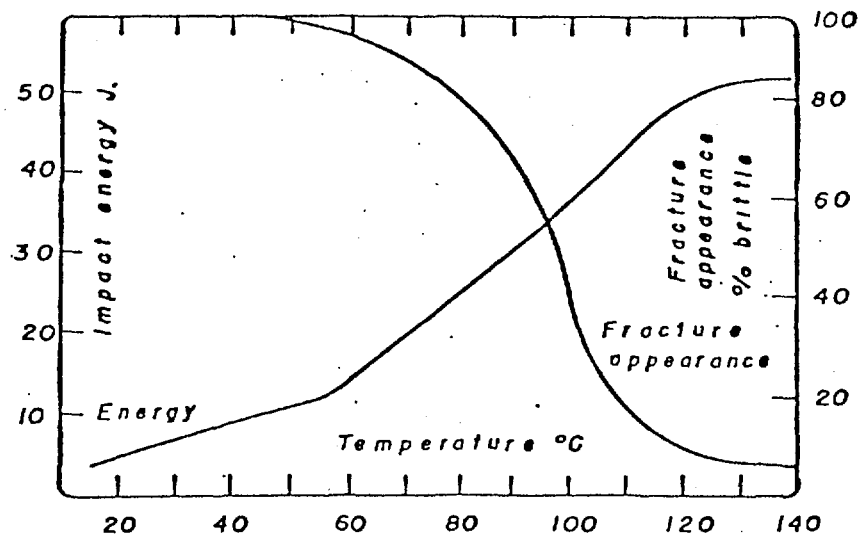


FIGURE 7 : Typical Charpy energy transition curve (V-steel). Ref. 12.

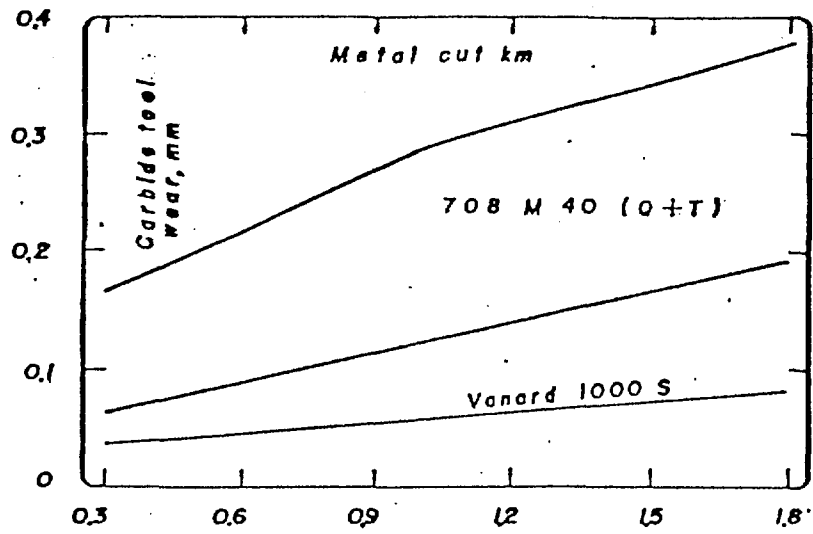


FIGURE 8 : Tool wear of vanard 1100S and 708M40 (EN 19). Ref. 12.

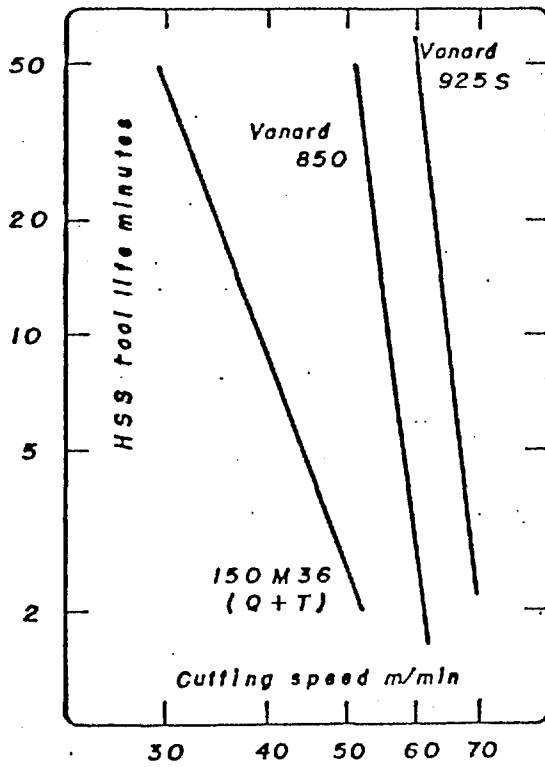


FIGURE 9 : Tool life, selected steels. Ref. 12.

HARDNESS (Hv)

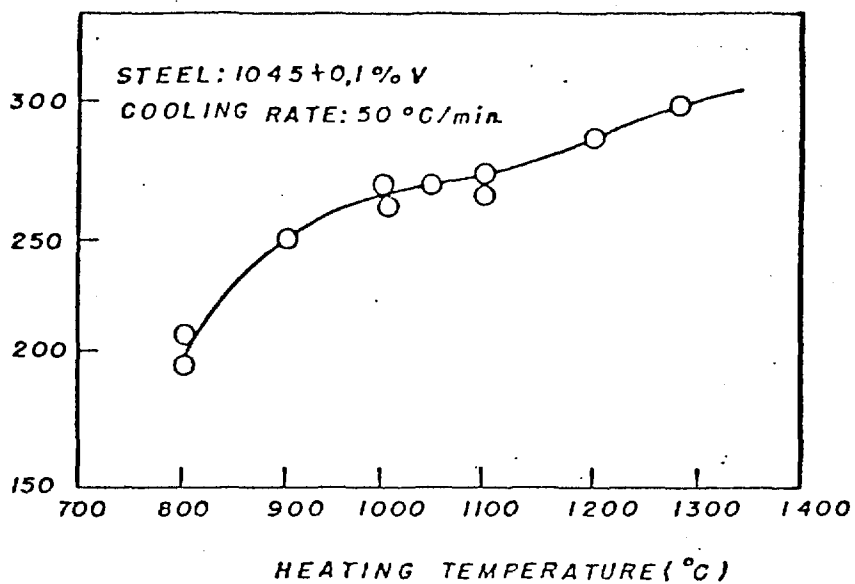


FIGURE 10 : The effect of heating temperature on the hardness of forgings. Ref. 10.

HARDNESS (Hv)

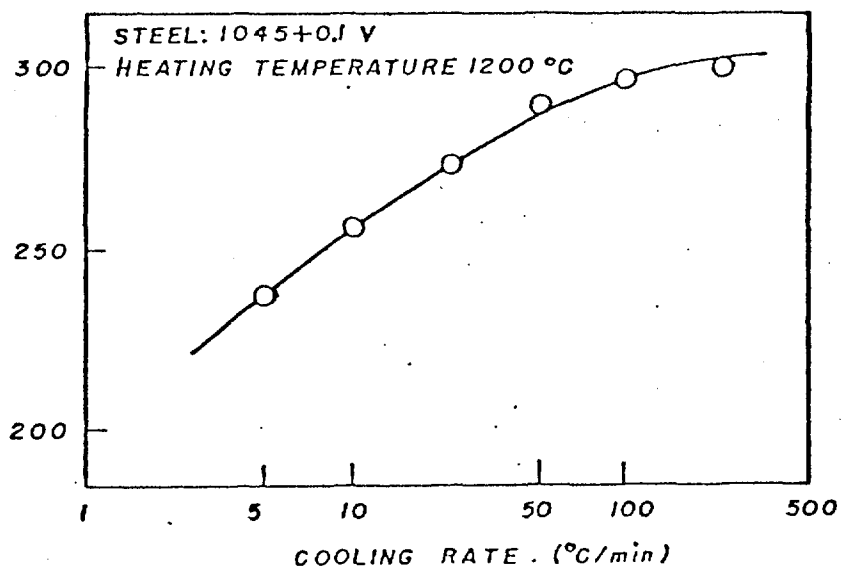


FIGURE 11 : Effect of cooling rate on the hardness of forgings. Ref. 10.

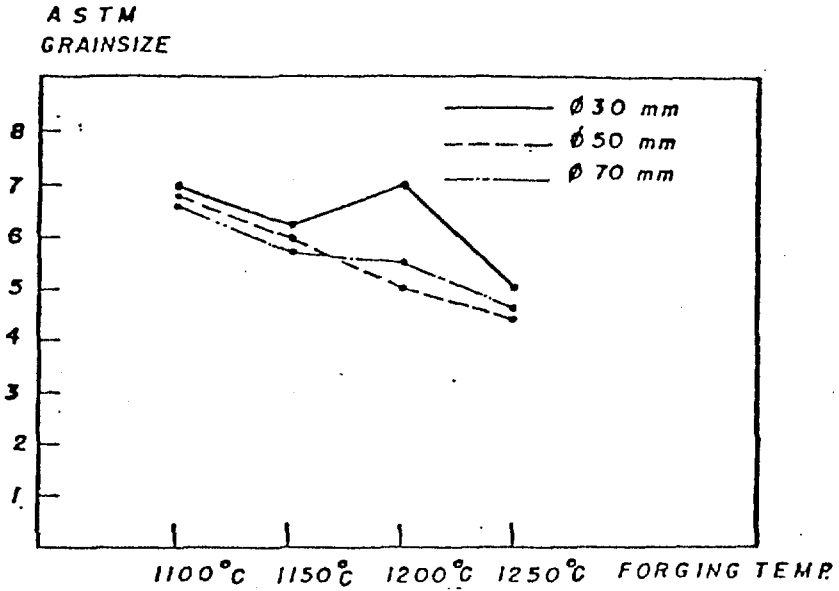


FIGURE 12 : Effect of forging temperature on the grain size of forgings. Ref. 9.

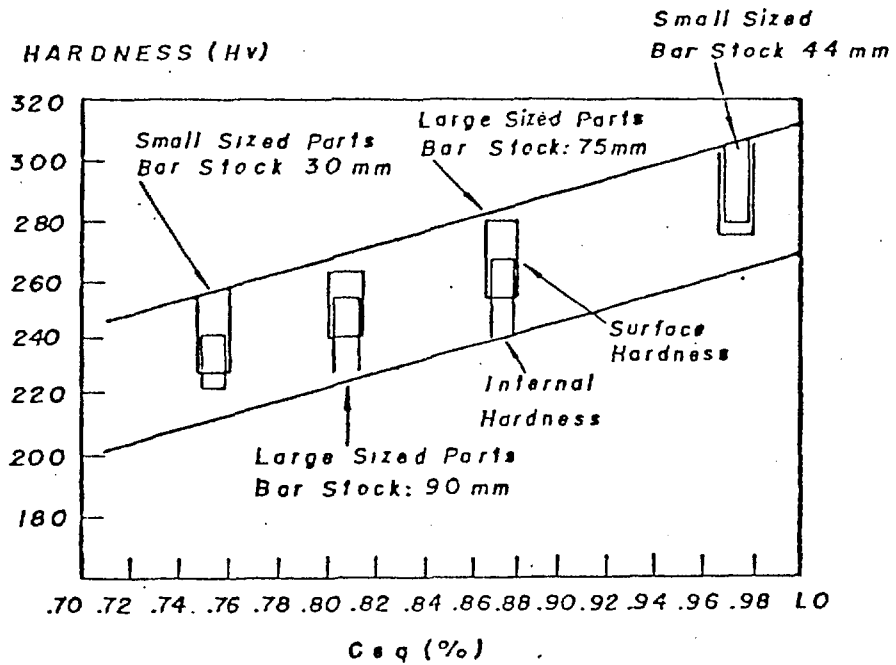
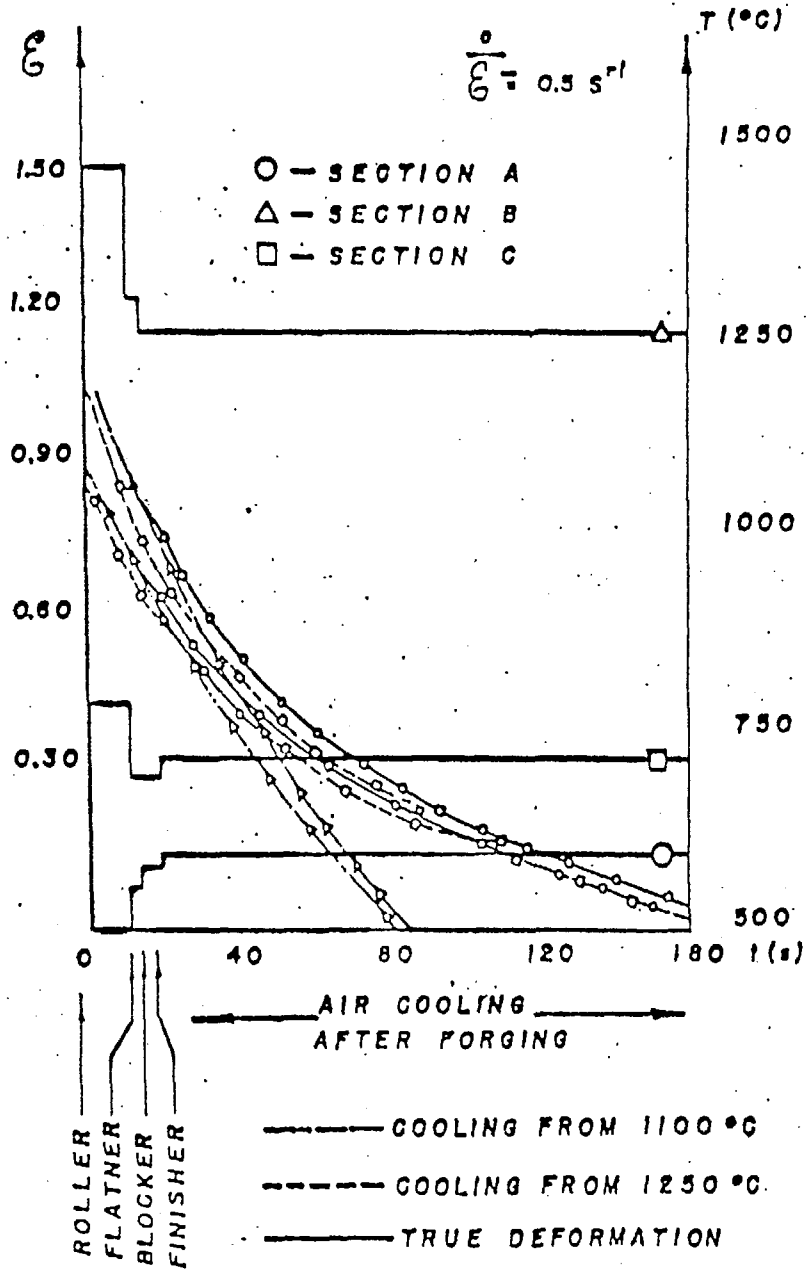


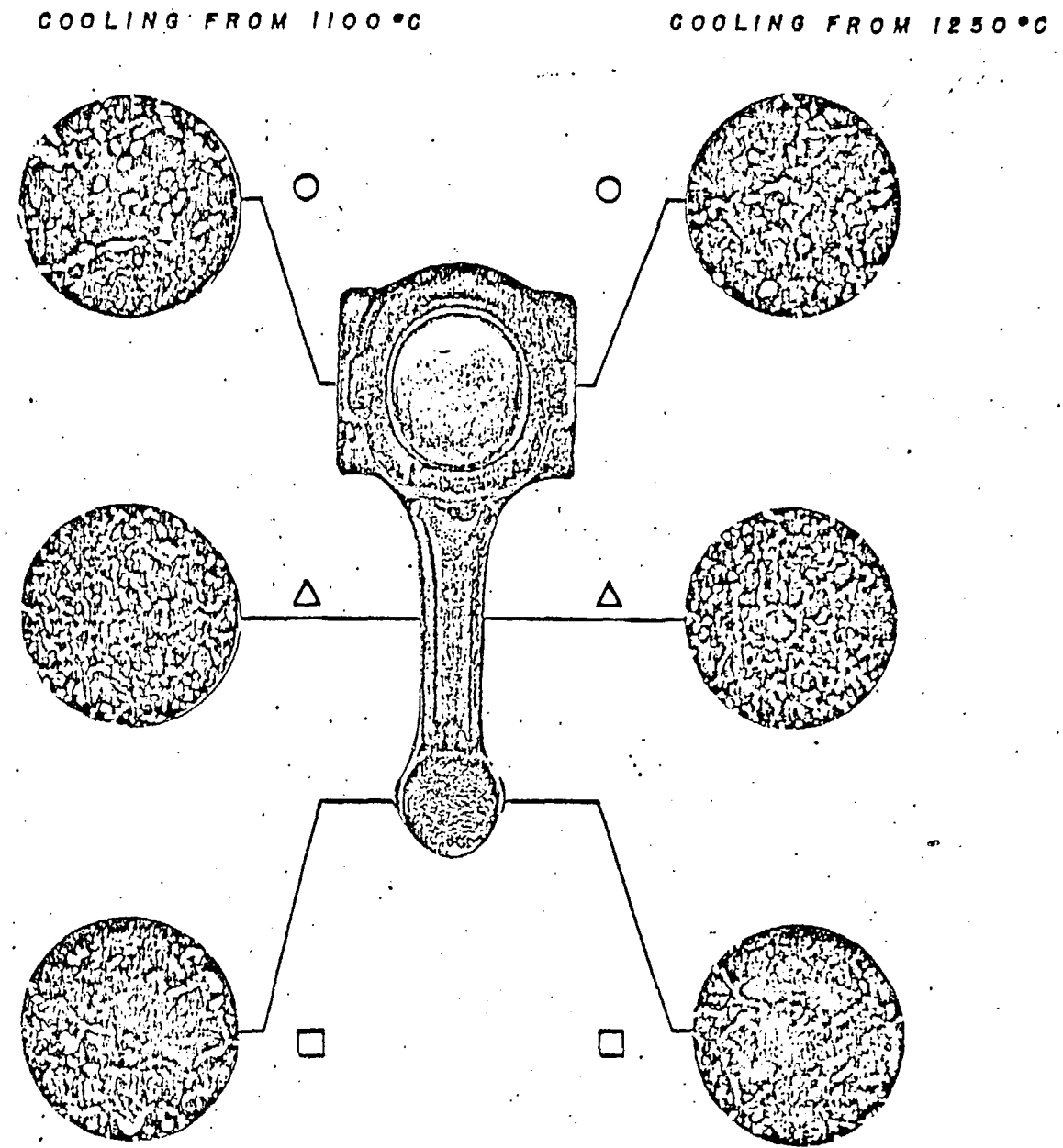
FIGURE 13 : Effect of carbon equivalent on the hardness. Ref. 13.

FIGURE 14

TYPICAL DEFORMATION AND TEMPERATURE PATH FOR CONNECTING ROD



STRUCTURE DISTRIBUTION FOR MAIN SECTIONS OF THE CONNECTING ROD (200 x)



VII - B - 29

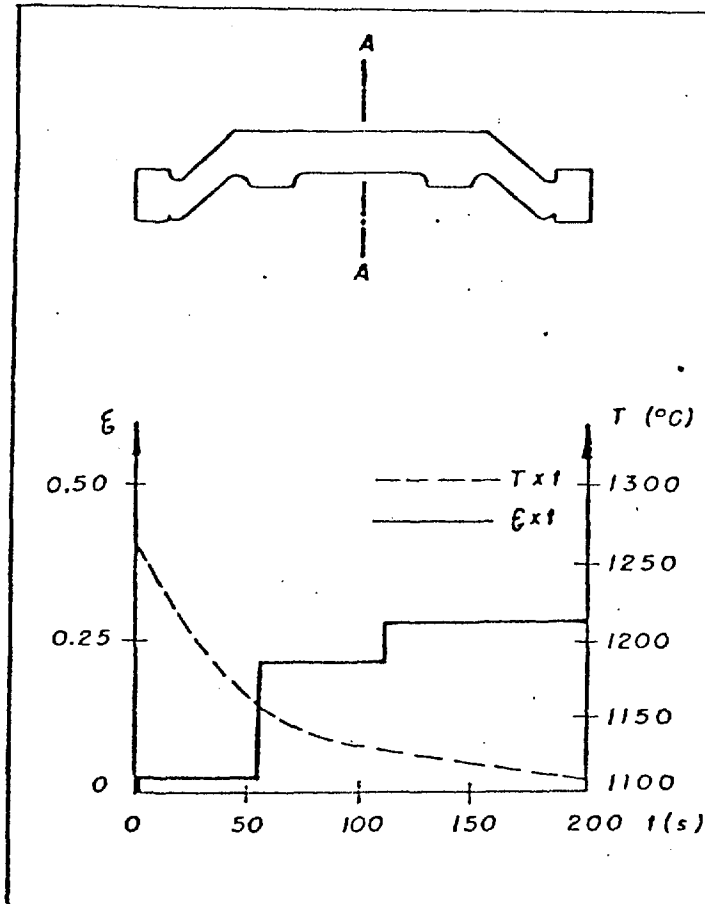
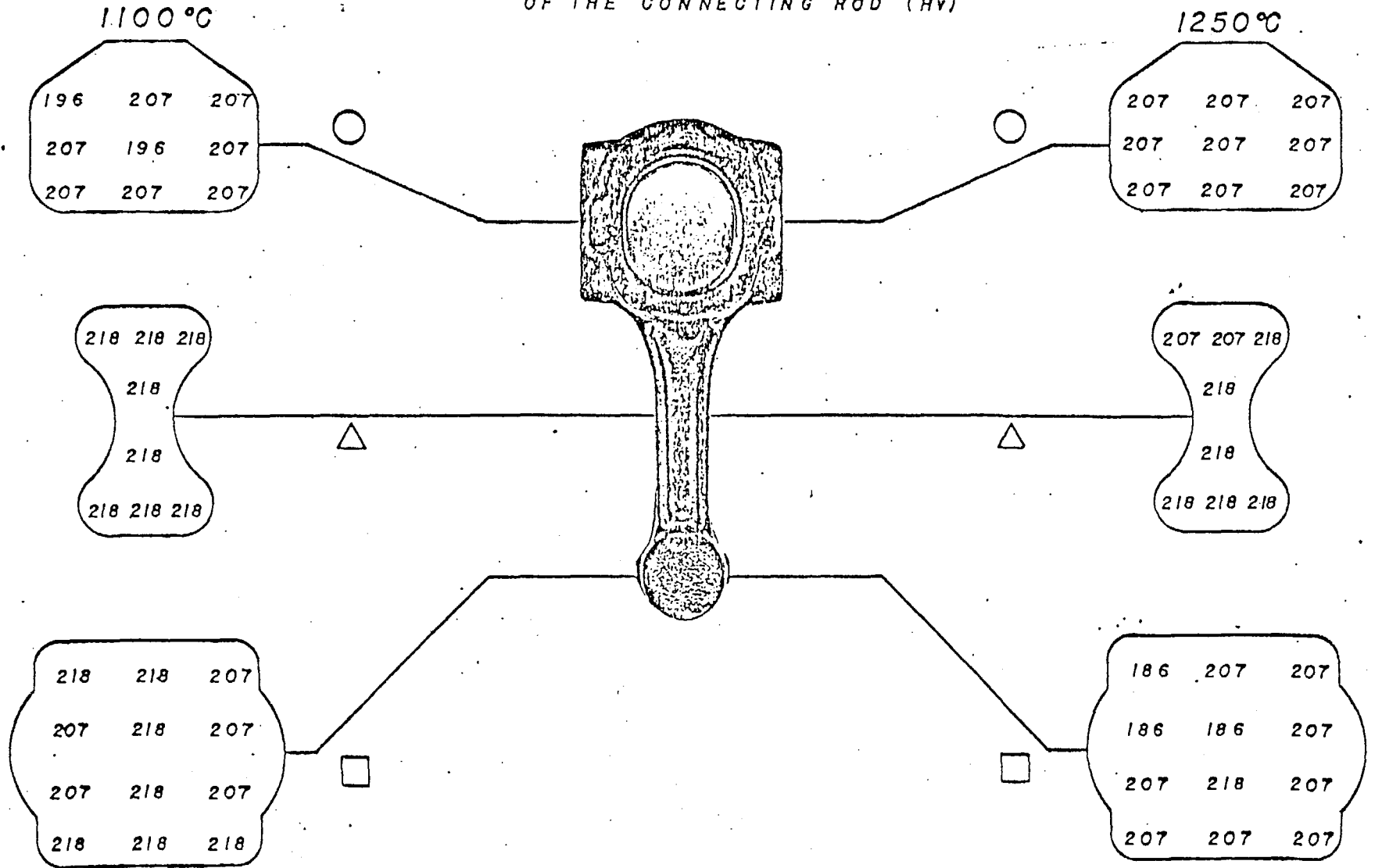


FIGURE 15 : Typical deformation and temperature path for the "A" section of the front axle.

FIGURE 16

HARDNESS DISTRIBUTION FOR MAIN SECTIONS
OF THE CONNECTING ROD (HV)



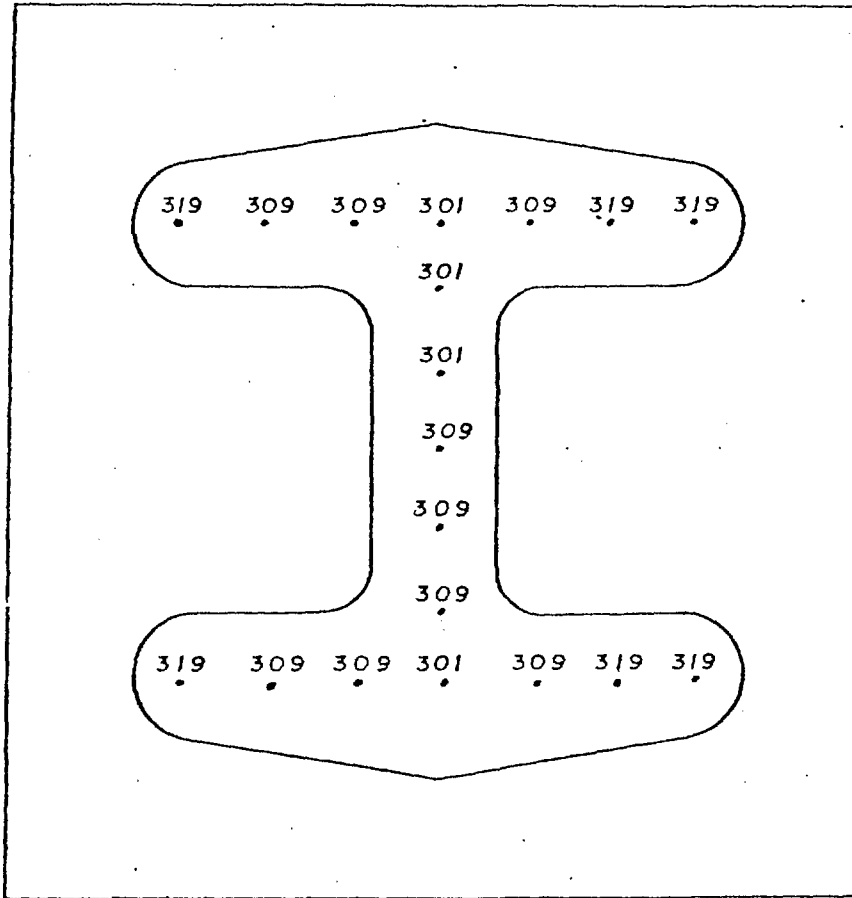
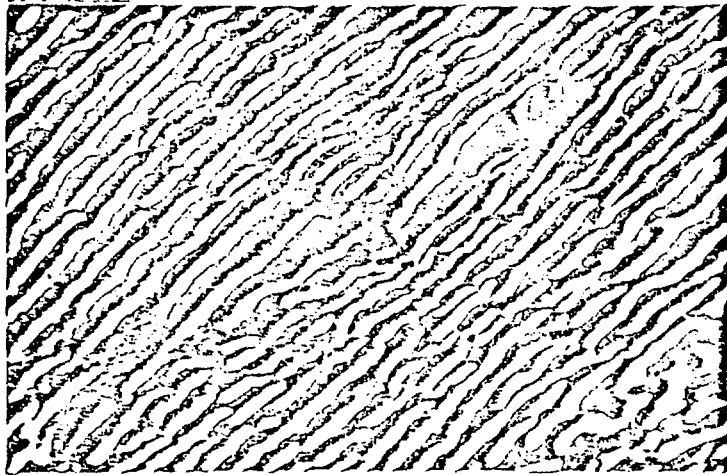
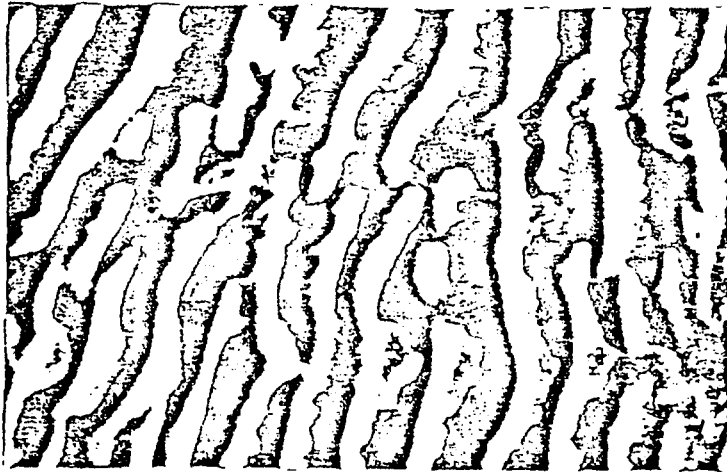


FIGURE 17 : Hardness distribution for section "A"
of the front axle (Hv).



(10000 x)

FIGURE 18 : Typical S.E.M. of pearlite



(20000 x)

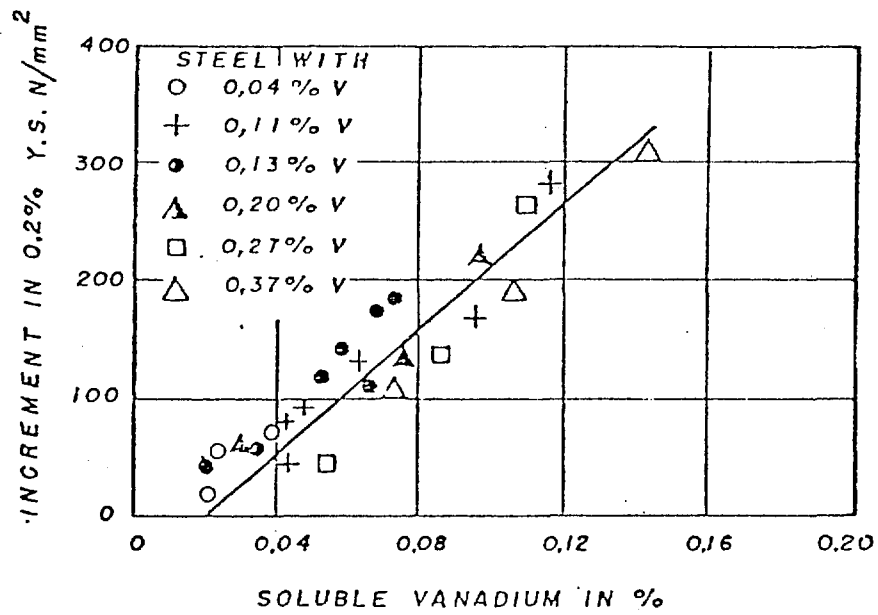


FIGURE 19 : Effect of Vanadium additions on 0,2% Y.S. Ref. 15